Organic & Biomolecular Chemistry

ROYAL SOCIETY OF CHEMISTRY

PAPER

View Article Online
View Journal

Cite this: DOI: 10.1039/d6ob00377j

Stereoselective synthesis of 1′-α-cyano carbocyclic pyrimidine nucleoside analogs *via* a chelation-controlled 1′-α-hydroxymethylation strategy

Nicolas. G. Biteau,† Mahesh Kasthuri,† Dharmeshkumar Patel, Ramyani De, Raymond. F. Schinazi* and Franck Amblard *

1′-α-Cyano nucleoside analogs have emerged as key structural motifs as antiviral agents. Due to their importance, we developed a novel stereoselective synthetic route to access 1′-α-cyano carbocyclic nucleoside analogs. The strategy relies on LDA-promoted chelation-controlled enolization, which favors a highly selective *Si*-face six-membered transition state with paraformaldehyde, delivering the exclusive 1′-α-hydroxymethylation product. This straightforward approach proceeds without the need for metal catalysts or additional promoters, highlighting its practicality and efficiency. The resulting 1′-α-hydroxymethylation intermediate enabled the synthesis of the desired 1′-α-cyano carbocyclic pyrimidine nucleoside analogs in a stereo controlled manner. This work represents the first example of such a selective and catalyst free access to these carbocyclic scaffolds.

Received 5th March 2026,
Accepted 27th April 2026

DOI: 10.1039/d6ob00377j

rsc.li/obc

Introduction

Modified nucleoside analogs have played a pivotal role in combating life-threatening viral outbreaks, including the recent COVID-19 pandemic caused by SARS-CoV-2.[1] While widespread vaccination has markedly reduced global mortality and morbidity, direct-acting antiviral agents have been indispensable in treating infected and hospitalized patients. Among them, RNA-dependent RNA polymerase (RdRp) inhibitors such as, approved nucleoside analogs Remdesivir (RDV)[2] and Molnupiravir[3] played a key role early on, despite some toxicity concerns,[4] modest clinical benefit, and, in the case of remdesivir, restriction to hospitalized patients due to its intravenous administration. Our group recently reported the discovery and evaluation of 1′-cyanocytidine (CNC) and its 5′-isobutyryl prodrug (CNiBuC) as promising anti-SARS-CoV-2 agents (Fig. 1a). CNC is a nontoxic nucleoside analog that exhibits submicromolar inhibition of SARS-CoV-2 replication in multiple cell-based assays and significantly reduces viral RNA levels and lung infectious virus titers in a Syrian hamster model. Intracellularly, CNC is metabolized to its active 5′-triphosphate form (CNC-TP), which targets the viral RNA-dependent RNA polymerase. Interestingly, CNC-TP does not cause stalling of replication like RDV instead we observed reversible competitive inhibition and impaired processivity that substantially reduces the replication of the viral genome. We also demonstrated that the 1′-cyano group plays a key role in countering the viral proofreading mechanism. Remarkably, the presence of the 1′-cyano modification in CNC, introduces a substantial kinetic barrier to this exonucleolytic excision, enabling the analog to evade proofreading and sustain its antiviral activity.[5]

On the other hand, carbocyclic nucleosides are a class of nucleoside analogs in which a methylene group replaces the furanose oxygen of the ribose or deoxyribose sugar. This structural modification confers enhanced chemical and metabolic stability by rendering the glycosidic bond resistant to cleavage by nucleoside phosphorylases and hydrolases.[6] As a result, carbocyclic nucleosides can display improved intracellular stability and pharmacokinetic properties.[7] Over the years, sustained efforts in the synthesis and evaluation of carbocyclic nucleoside analogs ultimately resulted in the approval of game-changer antivirals such as entecavir (HBV) or Abacavir (HIV) (Fig. 1a). Based on these observations, we hypothesized that synthesizing a carbocylic nucleoside incorporating CNC's key structural feature, namely it's 1′-CN group substitution, could further enhance its chemical properties and improve its overall antiviral efficacy.

Results and discussion

While the synthesis of CNC was relatively straightforward *via* a key silver triflate-mediated glycosylation of a 1-CN,1-Br riboside intermediate,[8] introduction of a cyano group at the 1′-position of carbocyclic nucleoside has never been reported

Center for ViroScience and Cure, Laboratory of Biochemical Pharmacology, Department of Pediatrics, Emory University School of Medicine, and Children's Healthcare of Atlanta, Atlanta, GA 30322, USA. E-mail: famblar@emory.edu
†NGB and MK, contributed equally to this work and should be regarded as co-first authors.

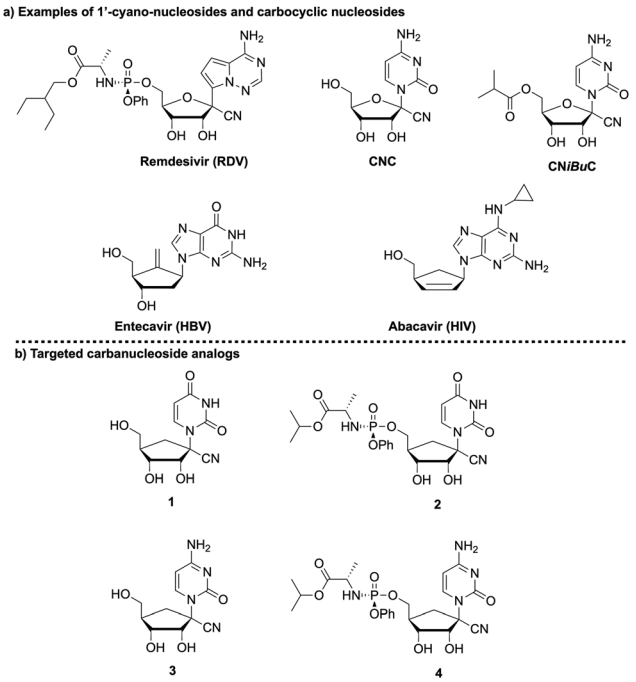

Fig. 1 (a) Known 1′-cyano-nucleoside inhibitors of SARCoV2 RdRp and FDA approved carbocylic nucleosides (b) targeted 1′-cyano-carbocyclic nucleoside analogs (**1–4**).

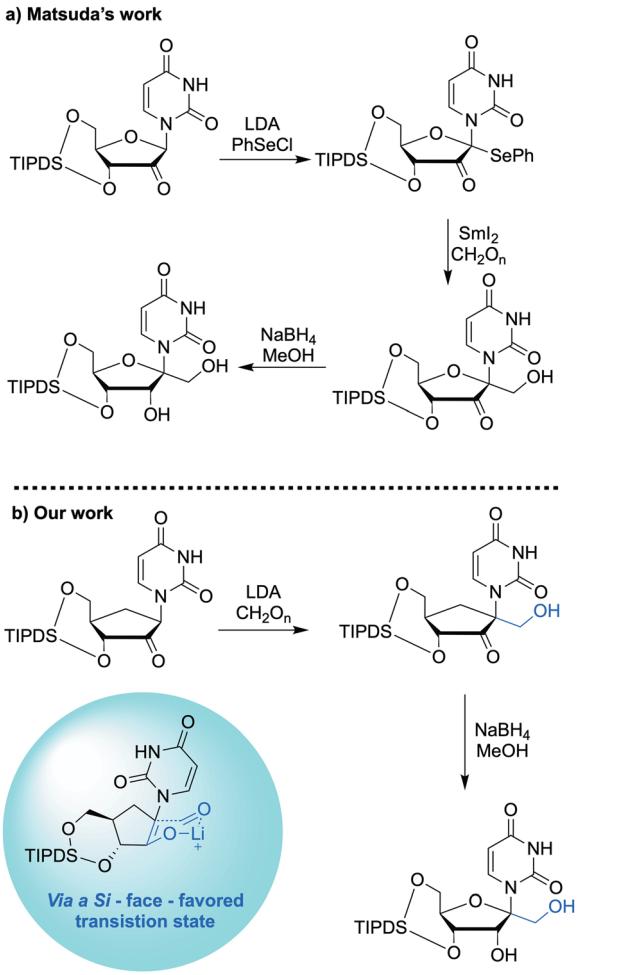

Scheme 1 (a) Previously reported stereoselective approach for 1′-α-hydroxymethylation of 2′-keto-uridine. (b) Present work: stereoselective route to 1′-α-hydroxymethylation of 2′-keto-carbocyclic uridine.

and only very few syntheses of 1′-modified carba-nucleosides have been described.[9]

In the ribose series, Matsuda and co-workers reported a highly stereoselective route to 1′-α-phenylseleno-2′-ketouridine derivatives, which served as key precursors for samarium diiodide-promoted aldol reactions. In their approach, reductive cleavage of the anomeric Se–C bond generated the corresponding samarium enolate, which underwent stereoselective condensation with aldehydes to furnish 1′-α-branched uridine analogs (Scheme 1a).[10] Inspired by this strategy and considering the absence of an anomeric center in our carbocyclic scaffold, we hypothesized that direct enolization with LDA followed by paraformaldehyde trapping could deliver α-selective functionalization at C1′ *via* a chelation-controlled transition state (Scheme 1b).

Accordingly, the starting 3′,5′-*O*-[tetraisopropyldisiloxane-1,3-diyl (TIPDS)]-2′-keto carbocyclic uridine **6** was prepared in 11 steps from (−)-Vince lactam **5**.[11] Treatment of **6** with LDA at −78 °C in THF, followed by addition of paraformaldehyde, afforded the desired 1′-hydroxymethylene-2′-keto carbocyclic uridine **7** as a single anomer in 50% yield. This yield represents the optimized outcome after systematic evaluation of different equivalents of LDA and paraformaldehyde, with the best result obtained using 8 equivalents of both reagents. At this stage, the stereochemistry of compound **7** could not be confirmed by NMR and attempts to obtain a crystal structure were unsuccessful. Therefore, the synthesis was continued and compound **7** was subsequently acetylated to afford compound **8** in 73% yield. Interestingly, reduction of carbo cyclic intermediate **8** using $NaBH_4$ in methanol at 0 °C afforded compound **9** in 76% yield as a single isomer, consistent with previously reported stereoselective reductions of ribose analogs (Scheme 2a). Compound **9** was finally protected by treatment with TBSOTf and 2,6-lutidine to furnish compound **10** in 86% yield.

With compounds **9** and **10** in hand, attempts were made to obtain crystals to confirm the 1′- and 2′-stereochemistry of the compound. Unexpectedly, X-ray analysis of crystals obtained from compound **9** by slow evaporation from methanol revealed a structure corresponding to the 2′-*O*-acetylated derivative **A**. Because the NMR of the compound **9** obtained after reduction was not compatible with the structure obtained *via* X-ray analysis, we hypothesized that the acetyl group migration[12] from the 1′-hydroxymethylene substituent to the adjacent 2′-hydroxy group occurred under the crystallization conditions (Scheme 2b). Despite this issue, the single-crystal X-ray structure of 2′-*O*-acetylated derivative **A** unambiguously confirmed the exclusive α-configuration of the 1′-hydroxymethylene substituent and the β-configuration of the 2′-hydroxyl group

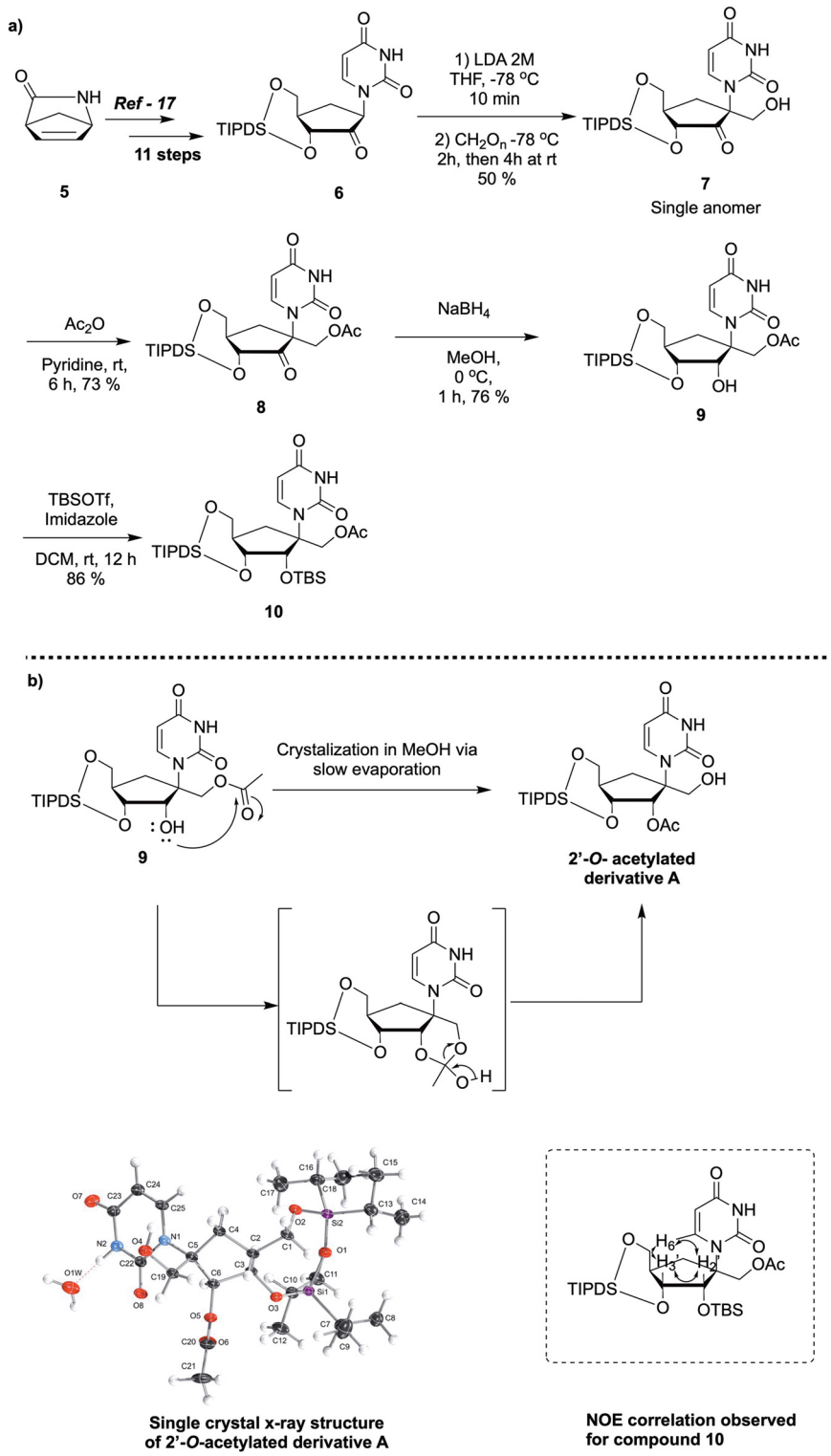

Scheme 2 (a) Synthesis of compound **10**. (b) Structural determination: single crystal X-ray structure of 2′-*O*-acetylated derivative obtained from compound **9** and NOE correlations observed for compound **10**.

obtained during the $NaBH_4$ reduction. In addition, the stereochemistry of fully protected compound **10** was confirmed by NOESY experiments, in which clear NOE correlations between nucleobase-H^6 proton and carba-sugar $H^{2'}$ protons were observed, validating the 1′- and 2′-stereochemistry of our intermediates (Scheme 2b).

Regarding the completely stereoselective 1′-α-hydroxymethylation, we postulated that the paraformalde-

hyde approach could occur either from the *Re* face or from the *Si* face of enolate **11** (Fig. 2). While a *Re*-face attack would lead to an unfavorable transition state (**13**), due to steric repulsion with the 5′-methylene moiety, a *Si*-face attack would allow the formation of a favorable six-membered transition state (**12**), likely dictating the stereochemical selectivity.

The targeted 1′-CN carba-uracil nucleoside (Carba-CNU-**1**) was finally obtained from compound **11** by first, treatment with NH_3 in MeOH to afford 1′-α-hydroxymethylene derivative **14**, followed by oxidation using Dess–Martin periodinane (DMP), hydroxylamine addition subsequent dehydration with $NaOAc/Ac_2O$ to give 1′-CN intermediate **16**. Final hydroxyls deprotection with TBAF afforded Carba-CNU-**1** in 80%. On the other hand, the targeted 1′-cyano carbocyclic cytidine analog (Carba-CNC-**3**) was synthesized by reacting Carba-CNU-**1** with Ac_2O and pyridine to afford tri acetylated compound **17** followed by conversion to the 4-triazolo intermediate **19** using $POCl_3$ and 1,2,3-triazole in the presence of Et_3N. Subsequent treatment with NH_4OH and final deprotection with NH_3/MeOH furnished Carba-CNC-**3** in 22% yield (Scheme 3).

In order to compete with natural nucleotides during viral RNA synthesis, nucleoside analogs must be activated by cellular kinases into their triphosphate forms.[13] However, inefficient first phosphorylation often limits their antiviral efficacy, particularly when non-ribose sugars (such as carbocyclic analogs) perturb sugar conformation and reduce kinase recognition.[14] To address this metabolic bottleneck, we adopted a commonly used phosphoramidate prodrug strategy, as seen in approved drugs such as sofosbuvir or remdesivir.[15] The lipophilic phosphoramidate moiety enhances cellular uptake and is enzymatically cleaved inside the cell to release the monophosphate intermediate,

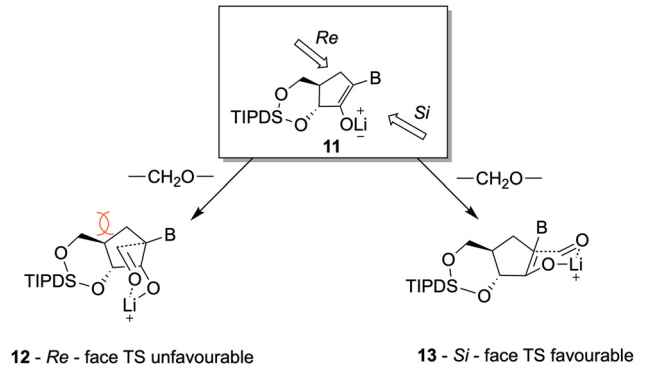

Fig. 2 Hypothesized transition state for the stereoselective hydroxymethylation of compound **6**.

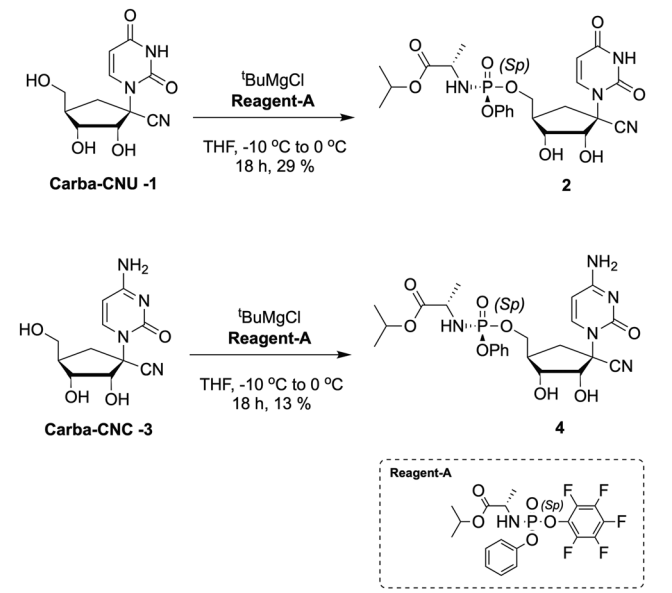

Scheme 4 Synthesis of phosphoramidate prodrugs **2** and **4**.

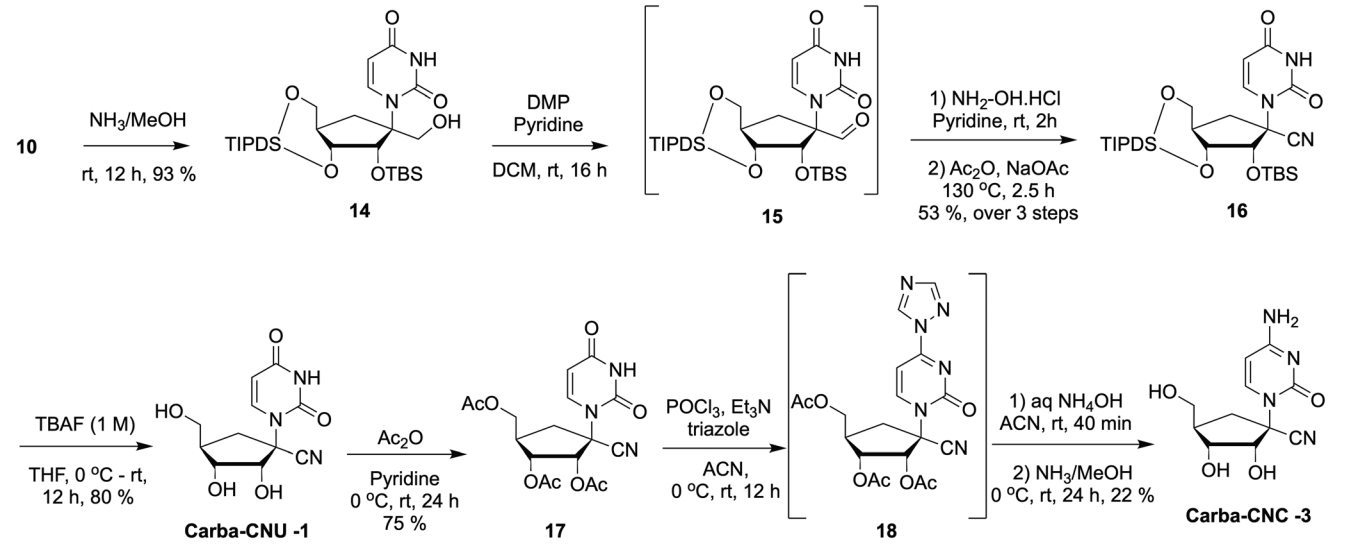

Scheme 3 Synthesis of 1′-cyano carbocyclic pyrimidine nucleoside Carba-CNU-**1** and Carba-CNC-**3**.

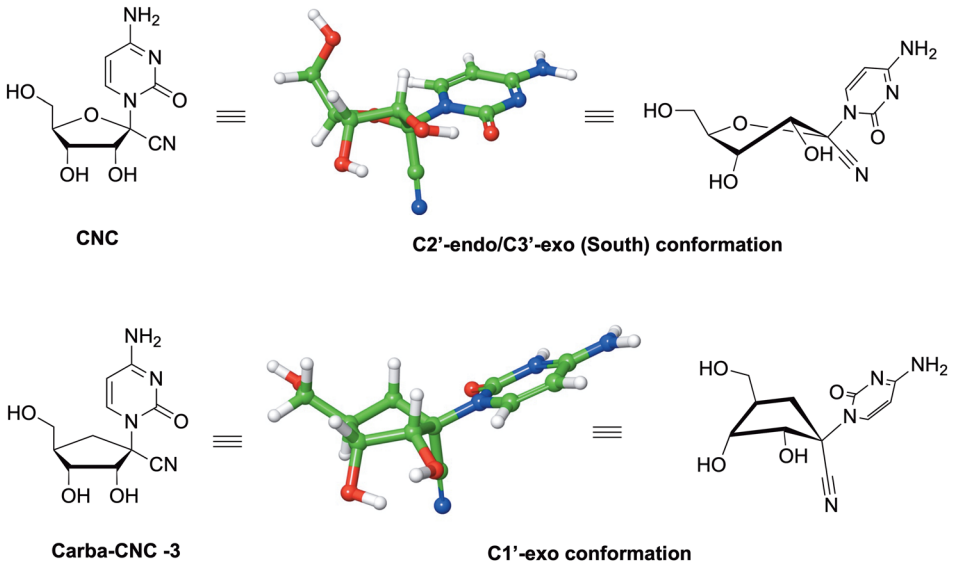

Fig. 3 Semiempirical and DFT-based geometry optimizations: CNC favors a C2′-*endo* conformation while Carba-CNC **3** favors a C1′-*exo* conformation.

thereby bypassing the rate-limiting kinase step and enabling more efficient formation of the active metabolite.[16] Thus, the corresponding phosphoramidate prodrugs **2** and **4** were synthesized in 7% and 13% yields respectively by treating either Carba-CNU-**1** or Carba-CNC-**3** in the presence of *tert*-butyl magnesium chloride and isopropyl ((*S*)-(perfluorophenoxy)-(phenoxy) phosphoryl)-L-alaninate in THF at 0 °C (Scheme 4).

Unfortunately, unlike CNC, which demonstrated potent dose-dependent anti-SARS-CoV-2 activity with EC_{50} values ranging from 0.6 to 2.1 μM across various tested cell lines,[5] neither Carba-CNU-**1**, Carba-CNC-**3**, nor their corresponding phosphoramidate prodrugs **2** and **4**, displayed antiviral activity against SARS-CoV-2 in Vero, Calu-3, and Caco-2 cell lines when tested up to 10 μM. Furthermore, compounds **1–4** were also screened against influenza A and B, Norovirus, Respiratory syncytial virus (RSV) and did not show any inhibitory activity at concentrations up to 40 μM (SI, Table S9). While replacement of the oxygen in the sugar ring by a methylene group improves the overall stability of what used to be the "glycosydic" bond, it can also lead to major conformation changes.[7] Indeed, the anomeric oxygen normally provides stabilizing *gauche* interactions with the 2′- and 3′-hydroxy groups, which are essential for maintaining the preferred sugar puckering in either the C2′-*endo*/C3′-*exo* (South) or C3′-*endo*/C2′-*exo* (North) forms. While both forms are known to be essential for antiviral activity,[17] the loss of these *gauche* interactions in carbocyclic nucleosides **1–4** may have led to a different and less preferable conformation. Using QM Conformer and Tautomer Predictor module within the Schrödinger Suite, we generated the low-energy conformers of CNC and Carba-CNC-**3** and compared their conformational landscapes.[18] This study revealed that CNC preferentially adopts a C2′-*endo*/C3′-*exo* (South) conformation, representing the lowest-energy structure among 80 predicted conformers, whereas Carba-CNC might exhibit its minimum-energy state in a 1′-*exo* conformation (Fig. 3), a conformation that could be associated with loss of activity in carbocyclic nucleosides. This difference in preferred sugar puckering between the two compounds, may represent one of the structural factors contributing to the observed loss of antiviral activity.

Conclusion

In summary, we report the first synthesis of 1′-α-cyano carbocyclic nucleoside analogs (**1–4**) *via* a practical and stereoselective LDA-promoted, chelation-controlled enolization strategy. This approach proceeds through a highly selective *Si*-face six-membered transition state with paraformaldehyde, affording the exclusive 1′-α-hydroxymethylation product without the need for metal catalysts or external promoters. Unfortunately, compounds **1–4** showed neither antiviral activity nor cytotoxicity in Vero, Calu3, or Caco2 cells when tested up to 10 μM. A comparative conformational analysis between CNC and Carba-CNC **3** revealed that Carba-CNC **3** might preferentially adopt a low-energy 1′-*exo* conformation, which may underline its lack of antiviral activity. The scope of this approach and its extension to other relevant electrophiles are currently being evaluated and will be reported elsewhere.

Author contributions

NGB and MK, contributed equally to this work and should be regarded as co-first authors. Conceptualization: FA, NB. Funding acquisition: FA, RFS. Resources: RFS. Data analysis: NGB, MK, RD, FA. Investigation: NB, MK. Computational data: DP. Supervision: FA, RFS. Writing of draft: MK. Writing: editing and review: FA, RFS.

Conflicts of interest

There are no conflicts to declare.

Data availability

The data supporting this article have been included as part of the supplementary information (SI). Supplementary information: procedures, characterization data, NMR spectra, X-ray crystal structure. See DOI: https://doi.org/10.1039/d6ob00377j.

CCDC 2521434 contains the supplementary crystallographic data for this paper.[19]

Acknowledgements

This work was supported by Emory's Center for AIDS Research (NIH grant P30-AI-050409). We thank Dr John Bacsa, Emory X-ray Crystallography Facility, for the X-ray structural analysis.

References

1 E.-I. Ami and H. Ohrui, Intriguing Antiviral Modified Nucleosides: A Retrospective View into the Future Treatment of COVID-19, *ACS Med. Chem. Lett.*, 2021, **12**, 510–517.

2 D. R. Martinez, F. R. Moreira, N. J. Catanzaro, M. V. Diefenbacher, M. R. Zweigart, K. L. Gully, G. de la Cruz, A. J. Brown, L. E. Adams, N. Catanzaro, B. Yount, T. J. Baric, M. L. Mallory, H. Conrad, S. R. May, S. Dong, D. T. Scobey, S. A. Montgomery, J. Perry, D. Babusis, K. T. Barrett, A. H. Nguyen, A. Q. Nguyen, R. Kalla, R. Bannister, J. P. Bilello, J. Y. Feng, T. Cihlar, R. S. Baric and R. L. Mackman, The Oral Nucleoside Prodrug GS-5245 Is Efficacious against SARS-CoV-2 and Other Endemic, Epidemic, and Enzootic Coronaviruses, *Sci. Transl. Med.*, 2024, **16**, eadj4504.

3 (*a*) R. M. Cox, J. D. Wolf and R. K. Plemper, Therapeutically administered ribonucleoside analogue MK-4482/EIDD-2801 blocks SARS-CoV-2 transmission in ferrets, *Nat. Microbiol.*, 2021, **6**, 11–18; (*b*) A. Jayk Bernal, M. M. Gomes da Silva, D. B. Musungaie, E. Kovalchuk, A. Gonzalez, V. Delos Reyes, A. Martín-Quiros, Y. Caraco, A. Williams-Diaz, M. L. Brown, A. Du, J. Pedley, C. Assaid, J. Strizki, J. A. Grobler, H. H. Shamsuddin, R. Tipping, H. Wan, A. Paschke, J. R. Butterton, M. G. Johnson and C. De Anda, Molnupiravir for Oral Treatment of Covid-19 in Nonhospitalized Patients, *N. Engl. J. Med.*, 2021, **386**, 509–520; (*c*) C. C. Lee, C. C. Hsieh and W. C. Ko, Molnupiravir-A Novel Oral Anti-SARS-CoV-2 Agent, *Antibiotics*, 2021, **10**, 1294.

4 (*a*) Y. S. Alsowaida, F. Shehadeh, M. Kalligeros and E. Mylonakis, Incidence and potential risk factors for remdesivir-associated bradycardia in hospitalized patients with COVID-19: A retrospective cohort study, *Front. Pharmacol.*, 2023, **14**, 1106044; (*b*) P. A. Escobar, Z. Sobol, R. R. Miller, S. Ferry-Martin, A. Stermer, B. Jacob, N. Muniappa, R. I. Sanchez, K. T. Blanchard, A. Galijatovic-Idrizbegovic, R. P. Amin and S. P. Troth, Comprehensive genotoxicity and carcinogenicity assessment of molnupiravir, *Toxicol. Sci.*, 2024, **202**, 278–290.

5 F. Amblard, M. Kasthuri, J. C. LeCher, S. Tao, R. De, R. Abdelnabi, I. Marko, L. Zhou, C. Li, J. Shi, S. L. Goh, J. Downs-Bowen, L. Bassit, S. Hurwitz, K. Zandi, T. McBrayer, B. Weynand, K. A. Johnson, J. Neyts and R. F. Schinazi, 1′-Cyanocytidine-5′-Isobutyryl Is a Potent SARS-CoV-2 Inhibitor in Culture and Infected Syrian Hamsters, *Sci. Adv.*, 2025, **11**, eadz5913.

6 M. K. Yates and K. L. Seley-Radtke, The Evolution of Antiviral Nucleoside Analogues: A Review for Chemists and Non-Chemists. Part II: Complex Modifications to the Nucleoside Scaffold, *Antiviral Res.*, 2019, **162**, 5–21.

7 (*a*) M. K. Yates and K. L. Seley-Radtke, The Evolution of Antiviral Nucleoside Analogues: A Review for Chemists and Non-Chemists. Part II: Complex Modifications to the Nucleoside Scaffold, *Antiviral Res.*, 2019, **162**, 5–21; (*b*) L. Agrofoglio, E. Suhas, A. Farese, R. Condom, S. R. Challand, R. A. Earl and R. Guedj, Synthesis of Carbocyclic Nucleosides, *Tetrahedron*, 1994, **50**, 10611–10670; (*c*) V. E. Marquez and M. I. Lim, Carbocyclic Nucleosides, *Med. Res. Rev.*, 1986, **6**, 1–40; (*d*) J. D. Stoeckler, C. Cambor and R. E. Parks, Human Erythrocytic Purine Nucleoside Phosphorylase: Reaction with Sugar-Modified Nucleoside Substrates, *Biochemistry*, 1980, **19**, 102–107; (*e*) J. B. Rodríguez and M. J. Comin, New Progresses in the Enantioselective Synthesis and Biological Properties of Carbocyclic Nucleosides, *Mini-Rev. Med. Chem.*, 2003, **3**, 95–114; (*f*) V. E. Marquez, Carbocyclic Nucleosides, *Adv. Antiviral Drug Des.*, 1996, **2**, 89–146.

8 T. A. Kirschberg, M. Mish, N. H. Squires, S. Zonte, E. Aktoudianakis, S. Metobo, T. Butler, X. Ju, A. Cho, A. Ray and C. U. Kim, Synthesis of 1′-C-Cyano Pyrimidine Nucleosides and Characterization as HCV Polymerase Inhibitors, *Nucleosides, Nucleotides Nucleic Acids*, 2015, **34**, 763–785.

9 (*a*) H. Li, W. Lee, J. C. Yoo and J. H. Hong, Selective synthesis of 1′(α), 2′(β)-C-dimethyl carbocyclic adenosine analogue as potential anti-HCV agent, *Bull. Korean Chem. Soc.*, 2009, **30**, 2039–2042; (*b*) P. Khirsariya, P. Pospíšil, L. Maier, M. Boudnÿ, M. Babáš, O. Kroutil, M. Mráz, R. Vácha and K. Paruch, Synthesis and Profiling of Highly Selective Inhibitors of Methyltransferase DOT1L Based on Carbocyclic C-Nucleosides, *J. Med. Chem.*, 2022, **65**, 5701–5723.

10 (*a*) T. Kodama, S. Shuto, S. Ichikawa and A. Matsuda, A Highly Stereoselective Samarium Diiodide Promoted Aldol Reaction with 1′ Phenylseleno 2′ Keto Nucleosides. Synthesis of 1′r Branched Uridine Derivatives, *J. Org. Chem.*, 2002, **67**, 7706–7715; (*b*) T. Kodama, A. Matsuda and S. Shuto, Synthesis of 1′-fluorouracil nucleosides as potential antimetabolites, *Tetrahedron*, 2006, **62**, 10011–10017; (*c*) T. Kodama, S. Shuto, M. Nomura and

A. Matsuda, An Efficient Method for the Preparation of 1′α-Branched-Chain Sugar Pyrimidine Ribonucleosides from Uridine: The First Conversion of a Natural Nucleoside into 1′-Substituted Ribonucleosides, *Chem. – Eur. J.*, 2001, **7**, 2332–2340; (*d*) T. Kodama, S. Shuto, M. Nomura and A. Matsuda, Synthesis of a 1′-α-phenylselenouridine derivative as a synthetic precursor for various 1′-modified nucleosides, via enolization at the 1′-position of 3′,5′-O-TIPDS-2′-ketouridine, *Tetrahedron Lett.*, 2000, **41**, 3643–3646.

11 (*a*) J. Liu, P. Wang, D. Nagarathnam, C. L. Espiritu, H. Bao, E. Murakami, P. A. Furman and M. J. Sofia, A 2′-Deoxy-2′-Fluoro-2′-C-Methyl Uridine Cyclopentyl Carbocyclic Analog and Its Phosphoramidate Prodrug as Inhibitors of HCV NS5B Polymerase, *Nucleosides, Nucleotides Nucleic Acids*, 2012, **31**, 277; (*b*) G. Birkus, O. Pav, T. Jandusik, I. Rosenberg and R. Nencka, *US Patent* 2019/0185510, 2019; (*c*) N. G. Biteau, S. A. Amichai, N. Azadi, R. De, J. Downs-Bowen, J. C. Lecher, T. MacBrayer, R. F. Schinazi and F. Amblard, Synthesis of 4′-Substituted Carbocyclic Uracil Derivatives and Their Monophosphate Prodrugs as Potential Antiviral Agents, *Viruses*, 2023, **16**, 544.

12 (*a*) R. Lassfolk and R. Leino, Mechanism of Acyl Group Migration in Carbohydrates, *Chem. – Eur. J.*, 2023, **29**, e202301489; (*b*) R. Lassfolk, S. Bertuzzi, A. Ardá, J. Wärnå, J. Jiménez-Barbero and R. Leino, Kinetic Studies of Acetyl Group Migration between the Saccharide Units in an Oligomannoside Trisaccharide Model Compound and a Native Galactoglucomannan Polysaccharide, *ChemBioChem*, 2021, **22**, 2986–2995; (*c*) L. Brecker, M. Mahut, A. Schwarz and B. Nidetzky, In Situ Proton NMR Study of Acetyl and Formyl Group Migration in Mono-O-acyl D-Glucose, *Magn. Reson. Chem.*, 2009, **47**, 328–332.

13 L. P. Jordheim, D. Durantel, F. Zoulim and C. Dumontet, Advances in the development of nucleoside and nucleotide analogues for cancer and viral diseases, *Nat. Rev. Drug Discovery*, 2013, **12**, 447–464.

14 (*a*) K. L. Seley-Radtke and M. K. Yates, The Evolution of Nucleoside Analogue Antivirals: A Review for Chemists and Non-Chemists. Part I: Early Structural Modifications to the Nucleoside Scaffold, *Antiviral Res.*, 2018, **154**, 66–86; (*b*) V. E. Marquez, Carbocyclic nucleosides, *Adv. Antiviral Drug Des.*, 1996, **2**, 89–146.

15 U. Pradere, E. C. Garnier-Amblard, S. J. Coats, F. Amblard and R. F. Schinazi, Synthesis of Nucleoside Phosphate and Phosphonate Prodrugs, *Chem. Rev.*, 2014, **114**, 9154–9218.

16 (*a*) Y. Mehellou, H. S. Rattan and J. Balzarini, The ProTide Prodrug Technology: From the Concept to the Clinic, *J. Med. Chem.*, 2018, **61**, 2211–2226; (*b*) M. Slusarczyk, M. Serpi and F. Pertusati, Phosphoramidates and Phosphonamidates (ProTides) with Antiviral Activity, *Antiviral Chem. Chemother.*, 2018, **26**, 1–31.

17 (*a*) E. W. Taylor, P. Van Roey, R. F. Schinazi and C. K. Chu, A Stereochemical Rationale for the Activity of Anti HIV Nucleosides, *Antiviral Chem. Chemother.*, 1990, **1**(3), 163–173; (*b*) K. Yamada, A. S. Wahba, J. A. Bernatchez, T. Ilina, S. Martínez-Montero, M. Habibian, G. F. Deleavey, M. Götte, M. A. Parniak and M. J. Damha, Nucleotide Sugar Pucker Preference Mitigates Excision by HIV-1 RT, *ACS Chem. Biol.*, 2015, **10**, 2024–2033.

18 (*a*) F. Molani and A. E. Cho, Accurate Protein Ligand Binding Free Energy Estimation Using QM/MM on Multi Conformers Predicted from Classical Mining Minima, *Commun. Chem.*, 2024, **7**, 247; (*b*) Y. Cao, T. Balduf, M. D. Beachy, M. C. Bennett, A. D. Bochevarov, A. Chien, P. A. Dub, K. G. Dyall, J. W. Furness, M. D. Halls, T. F. Hughes, L. D. Jacobson, H. S. Kwak, D. S. Levine, D. T. Mainz, K. B. Moore, M. Svensson, P. E. Videla, M. A. Watson and R. A. Friesner, Quantum Chemical Package Jaguar: A Survey of Recent Developments and Unique Features, *J. Chem. Phys.*, 2024, **161**, 052502.

19 CCDC 2521434: Experimental Crystal Structure Determination, 2026, DOI: 10.5517/ccdc.csd.cc2qmrlq.